

PACS numbers: 79.20.Ds; 79.20.Eb; 42.55.Rz
DOI: 10.1070/QE2013v043n03ABEH015106

Specific features of the behaviour of targets under negative pressures created by a picosecond laser pulse

S.A. Abrosimov, A.P. Bazhulin, V.V. Voronov, A.A. Geras'kin, I.K. Krasyuk, P.P. Pashinin, A.Yu. Semenov, I.A. Stuchebryukhov, K.V. Khishchenko, V.E. Fortov

Abstract. **New experimental data are obtained concerning the character of spallation and the mechanical strength of targets made of aluminium, aluminium–magnesium alloy (AMg6M), polymethylmethacrylate (PMMA, plexiglass), tantalum, copper, tungsten, palladium, silicon, and lead under the impact of laser radiation with the duration 70 ps. The specific features of the spallation phenomenon, in which the separation of a part of the target substance occurs at the back surface as a result of the effect of negative pressures (tensile stresses) in the substance, are experimentally studied. To determine the time moment of spallation, the electrocontact method of measuring the velocity of the spalled layer is developed and implemented. The obtained results show that the values of spall strength of the studied materials at moderate amplitudes of the shock-wave effect agree with the known literature data, while at higher pressures the growth of spall strength is observed, which is an evidence of the material hardening. The results of the studies demonstrate that the dynamic strength of a substance depends on both the duration and the amplitude of the shock-wave impact on the target.**

Keywords: *laser radiation, picosecond duration, ablation pressure, shock wave, negative pressure, spallation phenomenon, strain rate, ultimate strength, numerical modelling.*

1. Introduction

The interest in studying the substance in the region of negative pressures is related to the fact that it provides new data on the equations of state, phase transitions, polymorphous transformations, and mechanisms of material destruction under the tensile stresses in the regions of the phase diagram not studied before [1]. Currently the major interest is attracted by the shock-wave pico- and femtosecond-duration impact on studied targets, which allows advancing into the region of ultimately short-time tensile stresses.

The present paper reports the results of the study of the character of spallation and the dynamic mechanical strength of aluminium(Al), aluminium–magnesium alloy (AMg6M), polymethylmethacrylate (PMMA, plexiglass), tantalum (Ta), copper (Cu), tungsten (W), palladium (Pd), silicon (Si), and lead (Pb) targets irradiated by laser pulses with the duration 70 ps, when the material strain rate up to 4×10^8 s^{-1} is achieved.

To obtain the data on the dynamic mechanical strength of the studied materials, the spallation phenomenon was used, which occurs at the back (free) side of the target as a result of back-reflection of the pressure pulse, generated by the impact of the laser radiation pulse at the front surface of the target [2]. As a result of the reflection, the free surface of the target begins to move, which gives rise to the propagation of a wave of rarefaction in the opposite direction to the wave of compression. At a certain distance from the back surface the negative pressure (tensile stress) in the target may exceed the ultimate tensile strength of the material, giving rise to the formation of the spalled layer, which is separated and flies away from the initial sample. To determine the spall strength and strain rate of the material, we used the approach, based on measuring the depth of the resulting well, left by the spalled piece after the pulsed laser action on the target, and the velocity of the spalled layer with subsequent mathematical modelling of the shock-wave process within the studied target.

2. Experimental conditions

The experiments were carried out using the 'Camerton-T' setup at the A.M. Prokhorov General Physics Institute, RAS. The parameters of the setup were as follows: the active element was the neodymium phosphate glass, the operating wavelength was 0.527 μm (the second harmonic), and the pulse duration was 70 ps. The energy in the laser pulse was varied from 0.1 to 1.5 J. The output laser beam with the diameter 75 mm was focused by means of the two-component objective onto the targets into a spot with the diameter from 0.2 to 0.8 mm in correspondence with the target thickness, necessary to provide one-dimensionality of hydrodynamical flows in the studied samples. The intensity distribution of the laser radiation in the region of focusing was close to uniform. The maximal flow density of the laser radiation energy approached 6.2×10^{13} W cm^{-2}, and the ablation pressure attained 13.5 Mbar. The plates of the studied materials having the thickness from 50 to 380 μm were used as targets. The target materials were high-purity, except the palladium that contained some amount of carbon and oxygen impurity.

To determine the instant of the spallation event t_{sp}, which is important in the experiments with large amplitudes of shock-wave action, we used the electrocontact method of measuring the velocity of motion of the spalled layer [3]. In the general case in order to find the spallation instant t_{sp} it is necessary to use the nonlinear equation

S.A. Abrosimov, A.P. Bazhulin, V.V. Voronov, A.A. Geras'kin, I.K. Krasyuk, P.P. Pashinin, A.Yu. Semenov, I.A. Stuchebryukhov
A.M. Prokhorov General Physics Institute, ul. Vavilova 38, 119991 Moscow, Russia; e-mail: krasyuk@kapella.gpi.ru, lesha@kapella.gpi.ru;
K.V. Khishchenko, V.E. Fortov Joint Institute for High Temperatures, Russian Academy of Sciences, ul. Izhorskaya 13, Bld. 2, 125412 Moscow, Russia

Received 24 December 2012; revision received 8 February 2013
Kvantovaya Elektronika **43** (3) 246–251 (2013)
Translated by V.L. Derbov

$$t_{sp} + L/w_{sp} = t_1.$$

Here L is the spatial separation between the back side of the target and the electrocontact sensor (in our experiments L = 0.78 mm), and t_1 is the time, during which the spalled layer reaches the electrocontact sensor. The velocity of the spalled layer is calculated using the formula

$$w_{sp} = \frac{1}{m_{sp}} \int_0^{t_{sp}} P(t)\,dt,$$

where $P(t)$ is the profile of pressure in the plane of spallation, and $m_{sp} = \rho_0 h_{sp}$ is the mass of the spalled plate with the thickness h_{sp} per unit area. Numerical calculations show that during the free motion of the plate the shock-wave processes in it decay to zero, and the velocity of the plate can be characterised by its mean value w_{sp}. Under the conditions of the performed experiments the response time of the sensor t_1 was much greater than t_{sp}, so that the quantity $w_{sp} \approx L/t_1$ was accepted as the velocity of the spalled layer. Fixing the moment t_{sp} of spallation and knowing the plot of the dependence of pressure on time, one can determine the value of the spall strength $\sigma^* = |P(t_{sp})|$.

3. Numerical modelling

The calculations based on the experimental results were performed using the one-dimensional numerical code, implementing the scheme of the Courant–Isakson–Riess type, based on the equations of hydrodynamics [4]. In the calculations the wide-range semiempirical equations of the state of the studied substances were used [5, 6]. It was assumed that the shape of the ablation pressure pulse at the front surface of the target repeats the shape of the laser radiation pulse. The relation between the amplitude of the ablation pressure pulse P_a (in Mbar) and the intensity of laser radiation I_{las} (in TW cm^{-2}) was described by the semiempirical formula [7]:

$$P_a = 12(0.01 I_{las}/\lambda)^{2/3} [A/(2Z)]^{3/16},$$

which is applicable at $I_{las} \geqslant 1$ TW cm^{-2}. Here λ is the wavelength of the laser radiation (in μm); A is the atomic mass; and Z is the atomic number of the target substance.

In one part of experiments (the first type) the threshold intensity of the laser pulse, giving rise to the spallation, was recorded. In the other part of experiments (the second type), when the spallation threshold was exceeded, the major attention was paid to the velocity of the spalled layer, measured with the electrocontact sensor. Then for each experiment (in the framework of the hydrodynamic model) the calculations of the time dependences of pressure P and substance density ρ were performed at the position of the spallation plane, determined experimentally. The strain rate of the substance in the plane of spallation was found as the time derivative of the calculated function $\rho(t)$: $\dot{\varepsilon} = -\rho_0^{-1}(d\rho/dt)$, where ρ_0 is the initial density of the sample. In the plots presented below we used the equivalent recording of the strain rate, $\dot{\varepsilon} = V_0^{-1}(dV/dt)$, where $V = \rho^{-1}$ is the specific volume of the material, $V_0 = \rho_0^{-1}$. The results of one of the versions of numerical modelling of the laser radiation impact on the target made of 50-μm-thick aluminium are shown in Fig. 1. Note that, provided that the compression modulus B_0 is known for the studied material, the strain rate can be also calculated using the formula $\dot{\varepsilon} = B_0^{-1}(dP/dt)$, where $P(t)$ is the time dependence of pressure in the plane of spallation, determined by any available method.

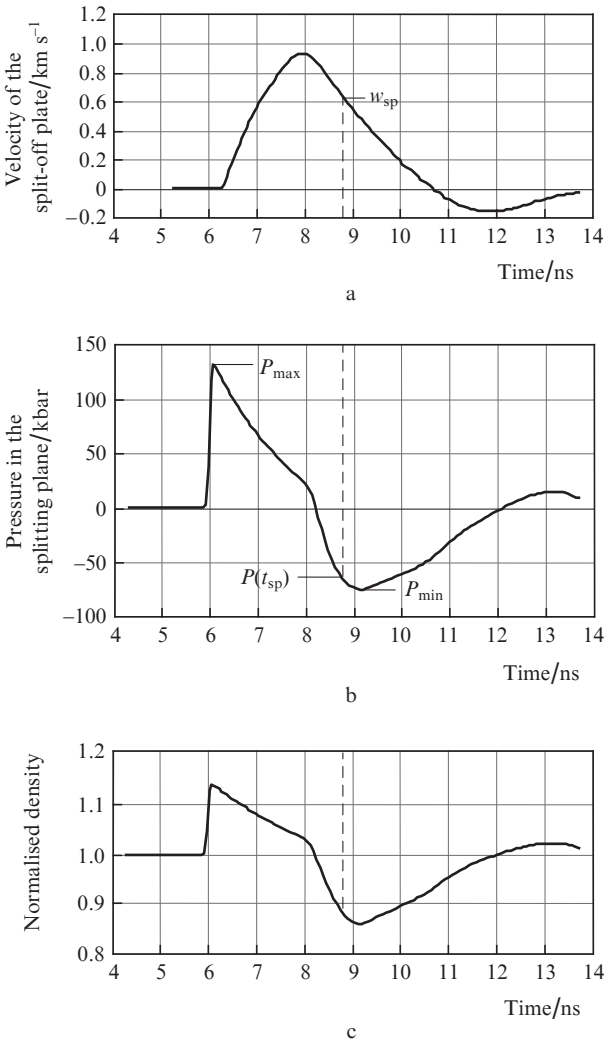

Figure 1. Calculated time dependences of the velocity of the spalled plate (a), the pressure (b), and the normalised density of material ρ/ρ_0 (c). The vertical dashed line corresponds to the moment of the spallation event.

In the first type of experiments at the threshold amplitudes of the shock impact the modulus of the minimal value of the negative pressure in the plane of spallation, $\sigma^* = |P_{min}|$, was taken for the value of the spall strength.

In the second type of experiments (at higher amplitudes of the shock impact) the value of the spall strength was determined using the measured velocity of the spalled layer w_{sp}, which allows determination of the time moment t_{sp} from the calculated time dependence of the spalled plate velocity (this velocity was estimated as the momentum of the plate, divided by its mass, with the position of spallation plane taken into account). In this case the spall strength was calculated as the modulus of the negative pressure at the moment of spallation, $\sigma^* = |P(t_{sp})|$ (see Fig. 1).

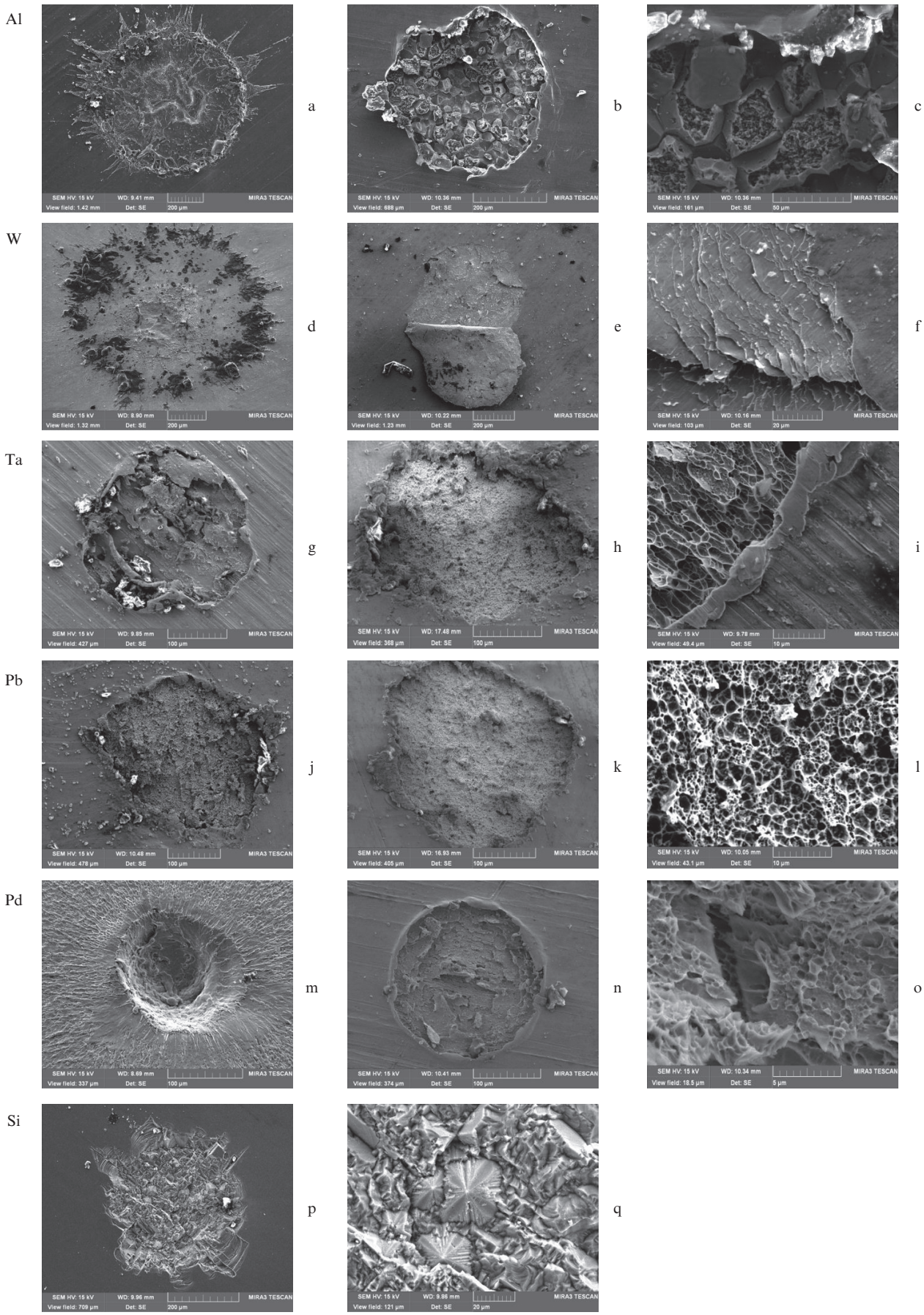

Figure 2. Differently magnified images of the front (a, d, m) and back (all the rest) surfaces of targets after laser impact, obtained by means of a scanning electron microscope of aluminium (a–c), tungsten (d–f), tantalum (g–i), lead (j–l), palladium (m–o), and silicon (p, q).

4. Results

Figure 2 shows the images of front and back surfaces of the targets after the impact of laser radiation with the duration of 70 ps. The photographs are obtained using a scanning electron microscope. We would like to draw attention to the images of the aluminium and tungsten targets. In the case of aluminium (Figs 2b, c) in the spallation plane one can see uniformly distributed formations, resembling the results of microexplosions in the spallation zone. Apparently, this is an evidence of inhomogeneities present in the substance [1]. In the case of tungsten in Fig. 2e (bottom) one can see the image of the spalled layer that was not separated from the target, while in Fig. 2f its layered structure is seen at the spallation boundary, which is an evidence of multiple spallation. The character of the spalled layer in the plates of silicon having the thickness 380 μm (Fig. 2q) with the orientation of the front face (100) (the angle deviation ±5°) seems like a result of melting in the spalled region followed by recrystallisation.

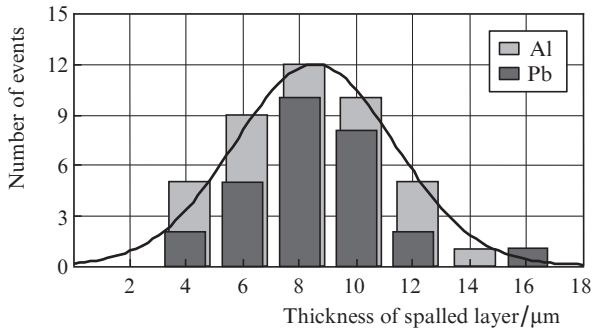

Figure 3. Histograms of the number of spallation events as a function of the spalled layer thickness for the targets made of aluminium and lead.

Figure 3 demonstrates the number of spallation events in aluminium and lead targets as a function of the thickness of the spalled layer. The distribution of the values is described by a Gaussian curve, which is an evidence of the random character of the spallation process.

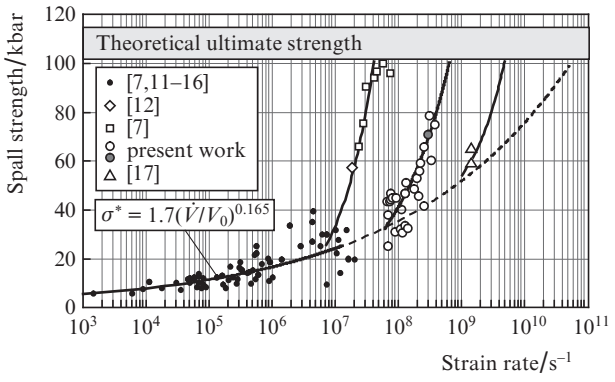

Figure 4. Spall strength σ^* of aluminium targets as a function of the strain rate $\dot{V}/V_0$ (experimental data) (● is the result of one of the experiments of the present work using the electrocontact sensor, see Fig. 1).

Figures 4–7 present the plots of the spall strength versus the strain rate for aluminium, alloy AMg6M, PMMA, tantalum, copper, and lead. For completeness of the picture and for comparison with the results of the present paper the data of experiments [8–19] are also presented.

From the analysis of Figs 5, 6 it is seen that in the case of aluminium, AMg6M and PMMA for the duration of the shock-wave action 1.5 and 2.5 ns, after a monotonic increase in the spall strength σ^* (explosion experiments), a significantly

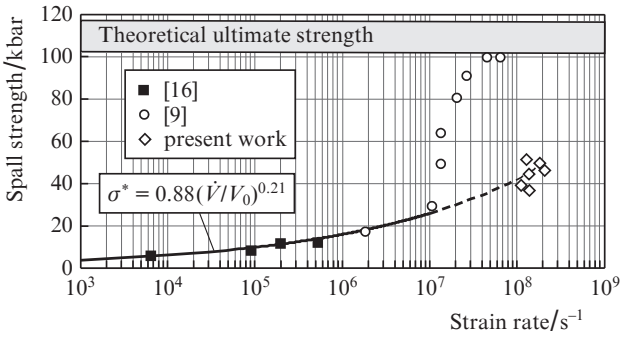

Figure 5. Spall strength σ^* of aluminium– magnesium alloy AMg6M targets as a function of the strain rate $\dot{V}/V_0$ (experimental data).

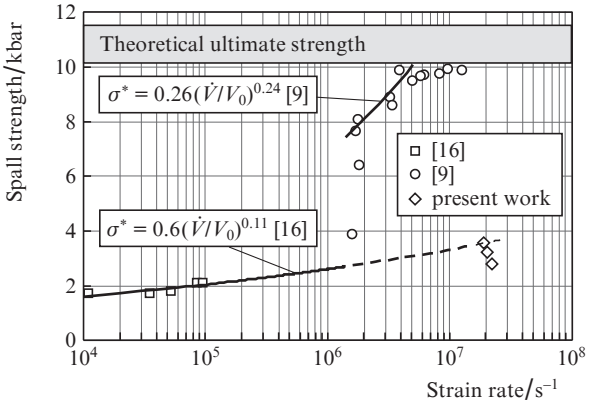

Figure 6. Spall strength σ^* of PMMA targets as a function of the strain rate $\dot{V}/V_0$ (experimental data).

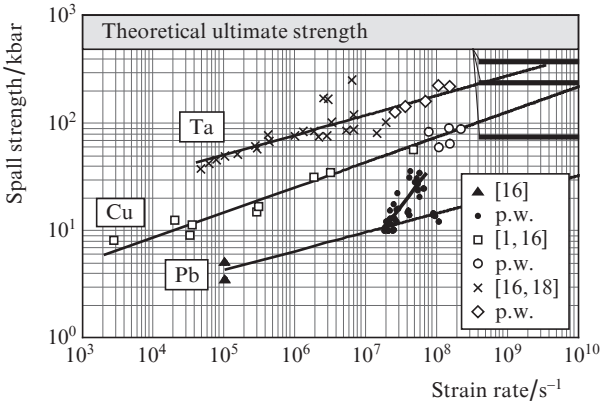

Figure 7. Spall strength σ^* of the lead, copper, and tantalum targets as a function of the strain rate $\dot{V}/V_0$ (experimental data).

faster growth of the strength up to the ultimate values occurs with further increasing the strain rate beyond a certain value. For aluminium the growth is observed in the range of rates $(1.4-4.4)\times10^7$ s^{-1}, for the alloy AMg6M $(1.0-4.0)\times10^7$ s^{-1}, and for PMMA – at 2.0×10^6 s^{-1}.

The values of the ultimate (ideal) strength were calculated using the formula

$$\sigma_{id} = -\rho_0 c_0^2/(4b),$$

where c_0 and b are the coefficients of the shock adiabatic curve of the material $D = c_0 + bu$ [20].

It is worth noting that the values of the ultimate strength, calculated in this way, are overestimated by nearly 20% as compared with the data of real semiempirical wide-range equations of the state [1].

The data, obtained under the impact of laser pulses with the duration 70 ps on the targets, show that at moderate amplitudes of the shock action the spall strengths are in agreement with the known functional dependences of these quantities on the strain rate. At higher pressure in the case of aluminium and lead (Figs 4 and 7) a rapid growth of the spall strength is observed, which indicates hardening of the materials as a result of shock impact. The registered growth of the spall strength in aluminium and lead is related to the fact that in the performed experiments the increase in the tension rate was achieved not only by reducing the duration of the impact, but also by increasing the amplitude of the shock action. The latter causes strengthening of the studied materials. In this case the material defects, giving rise to premature spallation, may vanish. This conclusion is confirmed by the results of the X-ray diffraction analysis of the aluminium and lead targets, performed using the DRON-4 diffractometer after the laser shock action. The study has shown that in such materials the modification of the crystal structure of the target material does not occur, and new phases do not appear. The broadening of X-ray diffraction lines is found, which evidences in favour of reduction of the crystal grain size. The appearance of the observed structure changes of the substance means that higher stresses are needed for the material breakdown, i.e., the ultimate strength of the material is increased [21], which is observed in the performed experiments.

As seen from Fig. 8, with increasing maximal pressure P_{max} in the spallation plane, the spall strengths of aluminium, alloy AMg6M and PMMA linearly increase until they attain theoretical strength limits. Figure 9 presents the dependences of the strain rate on P_{max} in the spallation plane according to the results of [7] and the present work. The presented data show that advancing towards higher strain rates requires either increasing the amplitude of the shock-wave action, or reducing its duration, which is more promising.

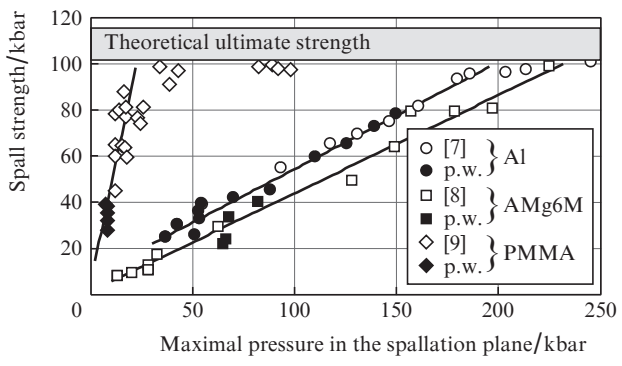

Figure 8. Spall strength σ^* as a function of the maximal pressure in the spallation plane P_{max} for aluminium, AMg6M, and PMMA (experimental data).

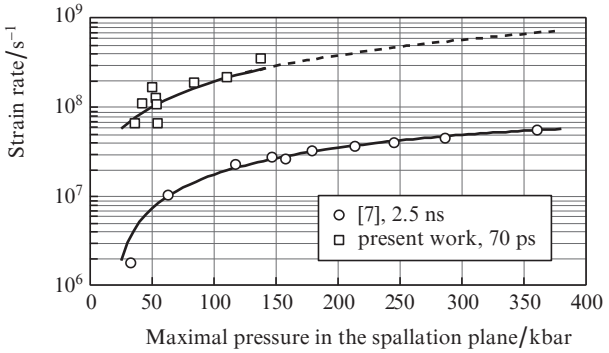

Figure 9. Strain rate $\dot{V}/V_0$ in aluminium targets as a function of the maximal pressure in the spallation plane P_{max} for the 2.5 ns [7] and 70 ps duration of shock impact upon the target.

5. Conclusions

In the present work the new data are obtained, concerning the strength of a number of materials under the conditions of high (up to 4×10^8 s^{-1}) strain rates. It is found that the behaviour of a substance under negative pressures strongly depends on the prehistory of the dynamic load, including many factors, among which an essential role is played by both the amplitude and the duration of the shock compression of the target. Beside the fundamental importance, the obtained results may find application in designing construction elements, operating under the conditions of highly concentrated energy impacts of small duration.

Acknowledgements. The authors thank A.I. Savvatimskii for offering a number of studied materials. The work was supported by the Russian Foundation for Basic Research (Grant Nos 11-02-12003-ofi_m-2011, 11-08-01225, 12-02-00625-a, and 12-02-00746-a), the programmes 'Extreme Light Fields and Their Applications' (No. 13P), and 'Matter at High Densities of Energy' (No. 2P) of the Presidium of RAS and by the President Grants for Government Support of the Leading Scientific Schools of the Russian Federation (Grant Nos NSh-368.2012.2 and No. NSh-7241.2012.2).

References

1. Kanel G.I., Fortov V.E., Razorenov S.V. *Usp. Fiz. Nauk*, **177** (8), 809 (2007) [*Phys.-Usp.*, **50** (8), 771 (2007)].
2. Zel'dovich Ya.B., Raizer Yu.P. *Physics of Shock Waves and High-Temperature Hydrodynamic Phenomena* (Mineola, New York: Dover Publications, 2002; Moscow: Fizmatlit, 2008).
3. Krasyuk I.K., Pashinin P.P., Semenov A.Yu., Fortov V.E. *Kvantovaya Elektron.*, **33** (7), 593 (2003) [*Quantum Electron.*, **33** (7), 593 (2003)].
4. Kulikovskii A.G., Pogorelov N.V., Semenov A.Yu. *Matematicheskiye voprosy chislennogo resheniya giperbolicheskikh sistem uravnenii* (Mathematical Problems of Numerical Solution of Hyperbolic Systems of Equations) (Moscow: Fizmatlit, 2012) p. 60.

5. Fortov V.E., Khishchenko K.V., Levashov P.R., Lomonosov I.V. *Nucl. Instr. Meth. Phys. Res. A*, **415** (3), 604 (1998).
6. Khishchenko K.V., Lomonosov I.V., Fortov V.E. *High Temp. High Press*, **30** (3), 373 (1998).
7. Abrosimov S.A., Bazhulin A.P., Voronov V.V., Krasyuk I.K., Pashinin P.P., Semenov A.Yu., Stuchebryukhov I.A., Khishchenko K.V. *Dokl. Akad. Nauk*, **442** (6), 752 (2012) [*Dokl. Phys.*, **442**, 64 (2012)].
8. Vovchenko V.I., Krasyuk I.K., Pasinin P.P., Semenov A.Yu. *Prikl. Fiz.*, **1**, 12 (2009).
9. Batani D., Vovchenko V.I., Kanel G.I., Kilpio A.V., Krasyuk I.K., Lomonosov I.V., Pasinin P.P., Semenov A.Yu., Fortov V.E., Shashkov E.V. *Dokl. Akad. Nauk*, **389** (3), 328 (2003) [*Dokl. Phys.*, **389**, 123 (2012)].
10. Geras'kin A.A., Khishchenko K.V., Krasyuk I.K., Pashinin P.P., Semenov A.Yu., Vovchenko V.I. *Contrib. Plasma Phys.*, **4** (7–8), 451 (2009).
11. Vovchenko V.I., Krasyuk I.K., Pashinin P.P., Semenov A.Yu. *Dokl. Akad. Nauk*, **338** (3), 322 (1994).
12. Moshe E., Eliezer S., Henis Z., Werdiger M., Dekel E., Horovitz Y., Maman S. *Appl. Phys. Lett.*, **76** (12), 1555 (2000).
13. Eliezer S., Gilath I., Bar-Noy T. *J. Appl. Phys.*, **67** (2), 714 (1990).
14. Fortov V.E., Kostin V.V., Eliezer S. *J. Appl. Phys.*, **70** (8), 4524 (1991).
15. Moshe E., Eliezer S., Dekel E., Ludmirsky A., Henis Z., Werdiger M., Goldberg I.B., Eliaz N., Eliezer D. *J. Appl. Phys.*, **83** (8), 4004 (1998).
16. Bachmann H., Baumung K., Kanel G.I., Karov H.U., Licht V., Rusch D., Singer J., Stoltz O. *Proc. 9th Int. Conf. High Power Particle Beams* (Springfield, VA: NTIS, 1993) Vol. 2, p. 963.
17. Kanel G.B., Razorenov S.V., Fortov V.E. *Shock-Wave Phenomena and Properties of Condensed Matter* (New York: Springer, 2004; Moscow: Yanus-K, 1996).
18. Ashitkov S.I., Agranat M.B., Kanel G.I., Komarov P.S., Fortov V.E. *Pis'ma Zh. Eksp. Teor. Fiz.*, **92** (8), 568 (2010) [*JETP Lett.*, **92** (8), 516 (2010)].
19. Razorenov S.V., Kanel G.I., Garkushkin G.V., Ignatova O.N. *Fiz. Tverd. Tela*, **54** (4), 742 (2012) [*Phys. Solid State*, **54** (4), 790 (2012)].
20. McQueen R.G., Marsh S.P. *J. Appl. Phys.*, **33**, 654 (1962).
21. Ionov V.N., Selivanov V.V. *Dinamika razrusheniya deformiruemogo tela* (Dynamics of Destruction of a Deformed Body) (Moscow: Mashinostroyeniye, 1987) p. 45.